

A Deep Convolutional Network to Extract Real-Time Landmarks for UAV Navigation

Osman Tokluoglu*, Mustafa Ozturk†

*Department of Electrical and Electronics Engineering, Ankara Yildirim Beyazit University, Ankara, Turkiye

†TAYF Research and Development Engineering Consulting Inc., Ankara, Turkiye

otokluoglu@aybu.edu.tr, mustafa@tayfargem.tr

Abstract—Recent advances in satellite and communication technologies have significantly improved geographical information and monitoring systems. Global System for Mobile Communications (GSM) and Global Navigation Satellite System (GNSS) technologies, which rely on electromagnetic signals transmitted from satellites and base stations, have long been utilized for geolocation applications. However, signal attenuation due to environmental conditions or intentional interference such as jamming may lead to severe degradation or complete loss of positioning capability. In such GNSS-denied environments, landmark extraction becomes critical for the navigation of unmanned aerial vehicles (UAVs) used in monitoring applications. By processing images captured from onboard UAV cameras, reliable visual landmarks can be identified to enable navigation without GNSS support. In this study, a convolution-based deep learning approach is proposed for the extraction of appropriate landmarks, and its effectiveness is examined.

Index Terms—FCN, GNSS, Landmark Extraction, ResNet, UAV Navigation, U-Net.

I. INTRODUCTION

Localization of unmanned aerial vehicles (UAVs) in regions where Global Navigation Satellite System (GNSS) signals are unavailable or insufficient is a significant challenge. In such environments, UAVs must be accurately positioned and be able to return to their initial takeoff point even without receiving localization signals. Although numerous methods have been proposed for UAV navigation in GNSS-denied environments [1]–[6], some studies [7], [8] employ deep learning approaches as a primary tool.

In the literature, landmark detection has been applied in various domains, such as robotic applications [9], [10], indoor navigation [1], and small-scale outdoor navigation [11]. Additionally, methods based on acoustic waves have also been proposed [12], [13]. However, many existing approaches [14]–[18] rely on photographic images for landmark extraction. In another study [19], Voronoi diagram segmentation was utilized to identify ground objects with geometric shapes as landmarks.

On the other hand, research specifically addressing the extraction of distinctive landmarks from aerial flight images for UAV navigation remains limited. Existing deep learning-based approaches applied to aerial imagery, such as [20], [21], are primarily designed for building segmentation tasks. Some building segmentation studies [22], [23] further incorporate adaptations that consider multi-scale features.

In this study, a fully convolutional network (FCN) architecture based on convolutional neural networks (CNNs) is

proposed for image-based UAV navigation. The proposed deep neural network architecture is trained to select distinctive landmarks from images captured along the UAV’s flight path. These landmarks are intended to be used for UAV navigation in conjunction with additional algorithms involving matching, searching, and route planning. In other words, this work focuses solely on extracting suitable landmarks that can serve as positioning control points for UAV navigation, while the aforementioned complementary algorithms are left for future research.

The proposed method aims to provide the following contributions to the literature:

- Investigating the impact on deep neural networks of selecting the number of kernels from the common elements of prime numbers and Fibonacci numbers,
- Developing a novel network architecture by employing the dilation method and residual (previous layer) connections, where dilation is applied only at the first stage and residual connections are incorporated exclusively at the second stage,
- Designing a network architecture that can be deployed on a real-time flying UAV by utilizing significantly fewer parameters and layers compared to well-known deep learning architectures.

The remainder of this paper is organized as follows. This section has presented general background information and a review of related work in the literature. In Section II, the solution approaches that influenced the development of the proposed method are discussed. Section II-A describes the dataset used for training the deep neural network, while Section II-B presents the details of the proposed method. A comparison of different approaches employed during the solution process and an evaluation of the proposed method are provided in Section III. Finally, the results are summarized in Section IV.

II. METHOD

This section describes the objective of the study and the methodology employed to achieve it, together with the underlying motivations. First, the rationale behind the selected approach is explained. Then, the dataset used for training is introduced, followed by a detailed description of the proposed method.

A. Approach

In this study, the objective is to extract distinguishable landmarks from images captured in areas where moving objects are minimal. The focus is on identifying landmarks from relatively static regions such as buildings and airport areas, which do not significantly change under varying environmental conditions throughout the day. Additionally, the extracted landmarks must be sufficiently distinct to avoid confusion with one another. The use of these landmarks primarily relies on images obtained from the downward-facing camera of the UAV during the training phase.

In [24], landmark extraction was investigated using relatively lightweight FCN architectures such as FCN-8, FCN-16, and FCN-32, where the numerical values indicate the upsampling factor. Another FCN-based architecture, U-Net [25], consists of downsampling, bottleneck, and upsampling stages. In this structure, features from previous layers are transferred to subsequent layers to enhance segmentation performance. The ResNet architecture proposed in [26], inspired by pyramidal neurons in the cerebral cortex, aggregates outputs from multiple layers, including skipped layers, to address the vanishing gradient problem. Although this structure mitigates gradient degradation and enables deeper networks, it increases overall network depth and parameter complexity.

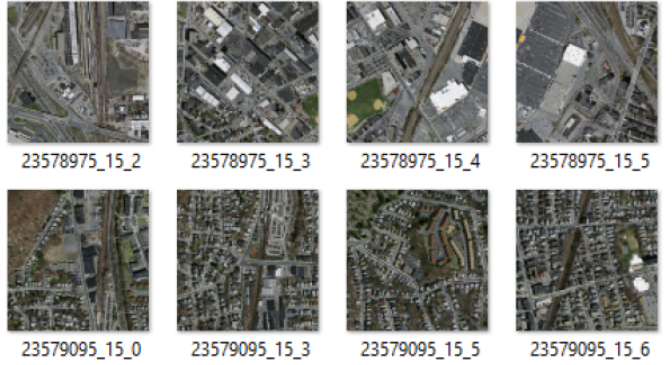
To improve the training speed of the proposed network, batch normalization is applied after convolution operations. Furthermore, dropout with rates of 0.1, 0.5, and 0.3 is employed in the 4th, 5th, and 6th activation layers, respectively, to regularize the network and activate a broader set of neurons. Spatial pooling is utilized during the expansion stage. In the first stage, a spatial pyramid structure is employed, followed by an FCN architecture similar to U-Net. In the final convolution layer, two additional layers with 1×1 kernel structures of the same size are appended.

Unlike conventional designs that typically select parameter and kernel numbers as powers of two, this study explores the use of special numerical sets such as Fibonacci numbers and prime numbers when determining the number of parameters and kernels.

B. Dataset and Training

For training the proposed network, the dataset introduced in [27], which contains segmented road and building images from the cities of Boston and Massachusetts, was utilized for landmark extraction. Instead of constructing a new dataset from scratch—a process that requires significant time and effort—the building segmentation dataset prepared by Mnih in [27] was adapted for training the proposed architecture.

From this originally unlabeled dataset, specialized structures such as lakes and buildings were selected to facilitate the training process. The original images, each with a resolution of 1500×1500 , were divided losslessly into nine equal sub-images of size 500×500 to make them compatible with the proposed network architecture. Following this partitioning process, images with unsuitable content were discarded. As a



(a) Sample aerial images from the dataset



(b) Corresponding ground-truth building segmentation maps

Fig. 1. The dataset used for network training was adapted from [27]. (a) Sample input aerial images; (b) corresponding ground-truth building segmentation maps.

result, the final dataset consisted of 600 training images, 63 validation images, and 26 test images.

Sample image pairs from the utilized dataset are shown in Fig. 1. While Fig. 1(a) presents the input aerial images, Fig. 1(b) illustrates the corresponding ground-truth building segmentation maps.

During the initial training phase, the Adam optimizer was employed with a learning rate of 0.005. The batch size was set to 200, and the number of epochs was chosen as 10.

C. Proposed Method

In the first stage, all convolutional layers employ the rectified linear unit (ReLU) activation function. The overall architecture of the proposed method, together with the activation function, is illustrated in Fig. 1. The network consists of a total of nine convolutional layers. After each convolution operation, batch normalization is applied up to the downsampling stage. Subsequently, the ReLU activation function is applied to the normalized feature maps.

The architecture follows a U-shaped structure. Downsampling operations are performed using max-pooling with identical pooling factors until the bottleneck layer is reached. After the initial expansion stage, specific numbers from a special numerical sequence—namely 3, 5, 13, 89, and 233—are

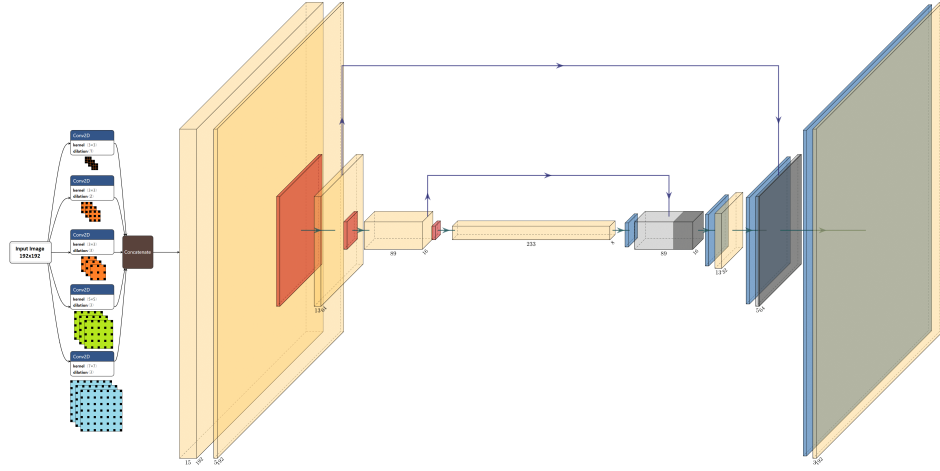


Fig. 2. Proposed deep convolutional neural network architecture. A 192×192 input image is processed through parallel convolutional branches with different kernel sizes and dilation rates to capture multi-scale representations. The concatenated feature maps are subsequently refined by hierarchical convolutional layers and compressed via a bottleneck structure for dimensionality reduction. Skip connections connect early and deeper layers to preserve spatial information and facilitate gradient propagation.

TABLE I
COMPARISON OF MODELS BASED ON TRAINING AND TEST RESULTS.

Method	Train/Test	Loss	Accuracy	IoU	Precision	Recall
Model 0 (Plain)	Train	0.1233	0.4948	0.1150	0.1045	0.0394
	Test	0.1599	0.3824	0.1108	0.1099	0.0289
Model 1 (Dilation)	Train	0.1245	0.5512	0.1158	0.1065	0.0380
	Test	0.1833	0.4877	0.1304	0.1518	0.0566
Model 2 (Residual)	Train	0.1176	0.5504	0.1304	0.1473	0.0823
	Test	0.1734	0.4877	0.1381	0.2202	0.0862
Proposed Method	Train	0.1146	0.4946	0.1347	0.1568	0.0909
	Test	0.1468	0.3824	0.1324	0.1721	0.0803

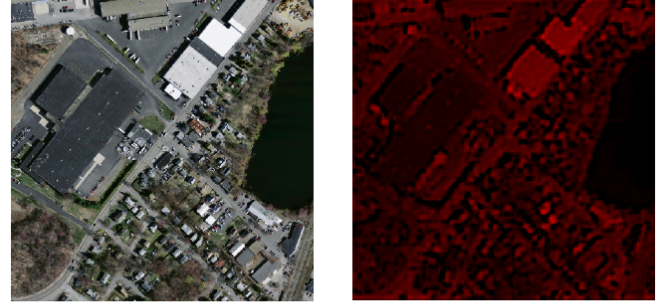
assigned as channel numbers. The first convolutional layer contains 5 channels, while the subsequent layers contain 23, 89, and 233 channels, respectively.

The proposed architecture can be conceptually divided into two phases. In the first phase, each dilation layer employs three kernels with distinct dilation rates derived from a predefined numerical sequence. In the second phase, a modified U-Net structure is constructed with additional skip connections to enhance feature propagation and segmentation performance.

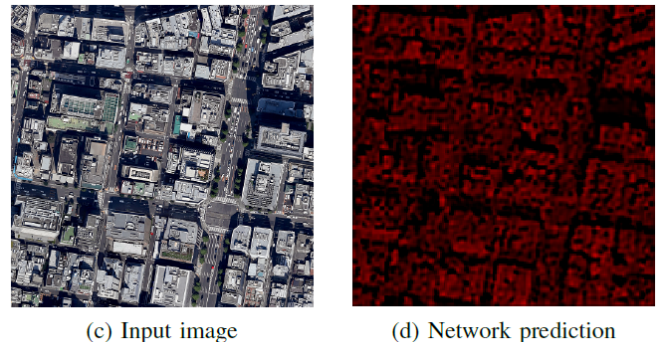
III. RESULTS AND DISCUSSION

Four different approaches, including the proposed method, were trained using the constructed dataset, and their results are presented in Table I. The first model consists solely of convolutional layers and pooling operations. In this structure, batch normalization is applied after each convolutional layer. Additionally, dropout is employed after selected layers. This baseline model is referred to as “Model 0 (Plain)”.

In the second model, dilation layers with various kernel types and dilation rates are incorporated into Model 0 as the first stage, forming “Model 1 (Dilation)”. In the third approach, residual connections are added to Model 0, enabling information from previous layers to be propagated to deeper layers. This structure is referred to as “Model 2 (Residual)”.



(a) Input image (b) Network prediction



(c) Input image (d) Network prediction

Fig. 3. The input images shown in (a) and (c) were used to evaluate the proposed method. The corresponding output predictions obtained from the network are presented in (b) and (d).

Finally, in the proposed method, both dilation and residual connections are integrated into the baseline architecture. As illustrated in Fig. 2, the network structure is completed by combining these two mechanisms. After training the models as described in the dataset and training section, the performance metrics summarized in Table I were obtained.

As shown in Fig. 3, the proposed model was evaluated using real aerial images, and the results presented in Fig. 3(b) and Fig. 3(d) were obtained. Although water, road, or land areas are not explicitly highlighted in the predictions, this does not necessarily indicate that the proposed network performs sufficiently well. Moreover, training with a batch size of 200 and only 10 epochs may not be adequate to achieve optimal performance. The effect of input size was also investigated in this study. When the input size was doubled, no significant improvement in the results was observed. Therefore, 192×192 was retained as the default input image size. Convolution operations were performed using padding in order to preserve spatial dimensions, which may lead to information loss around the image boundaries. Employing valid padding instead of same padding could potentially improve performance. These aspects will be considered in future work. Additionally, incorporating two- and three-layer convolutional blocks may further enhance the overall performance of the proposed architecture.

IV. CONCLUSION

This study proposed a novel FCN-based segmentation framework for landmark extraction in GNSS-denied environments to enable UAV localization using downward-facing camera imagery. In the absence of a dedicated UAV landmark dataset, the model was trained on existing UAV and satellite-based building segmentation datasets. Despite dataset and training constraints, the results demonstrate the feasibility of transferring segmentation knowledge to landmark extraction, with further gains expected from larger datasets and extended training. Future work will focus on architectural refinements and optimized training to enhance generalization. The lightweight architecture supports real-time embedded deployment, and FPGA implementation with quantization and pruning will be explored for low-latency, energy-efficient onboard processing. Overall, the framework lays a foundation for vision-based UAV navigation and future algorithmic and hardware improvements.

REFERENCES

- [1] F. J. Perez-Grau, R. Ragel, F. Caballero, A. Viguria, and A. Ollero, “An architecture for robust UAV navigation in GPS-denied areas,” *Journal of Field Robotics*, vol. 35, no. 1, pp. 121–145, 2018.
- [2] Y. Lu, Z. Xue, G.-S. Xia, and L. Zhang, “A survey on vision-based UAV navigation,” *Geo-Spatial Information Science*, vol. 21, no. 1, pp. 21–32, 2018.
- [3] G. Balamurugan, J. Valarmathi, and V. P. S. Naidu, “Survey on UAV navigation in GPS denied environments,” in *Proc. 2016 Int. Conf. Signal Processing, Communication, Power and Embedded System (SCOPES)*, 2016, pp. 198–204.
- [4] G. Hemann, S. Singh, and M. Kaess, “Long-range GPS-denied aerial inertial navigation with LIDAR localization,” in *Proc. 2016 IEEE/RSJ Int. Conf. Intelligent Robots and Systems (IROS)*, 2016, pp. 1659–1666.
- [5] S. Singh and P. B. Sujit, “Landmarks based path planning for UAVs in GPS-denied areas,” *IFAC-PapersOnLine*, vol. 49, no. 1, pp. 396–400, 2016.
- [6] O. Tokluoglu and E. Cavus, “Study of utilizing multiple IMUs for inertial navigation systems without GPS aid,” in *Proc. 2019 1st Global Power, Energy and Communication Conf. (GPECOM)*, Nevsehir, Turkiye, 2019, pp. 86–89.
- [7] J. R. G. Braga, H. F. C. Velho, G. Conte, P. Doherty, and É. H. Shiguemori, “An image matching system for autonomous UAV navigation based on neural network,” in *Proc. 2016 14th Int. Conf. Control, Automation, Robotics and Vision (ICARCV)*, 2016, pp. 1–6.
- [8] H. Goforth and S. Lucey, “GPS-denied UAV localization using pre-existing satellite imagery,” in *Proc. 2019 Int. Conf. Robotics and Automation (ICRA)*, 2019, pp. 2974–2980.
- [9] M. Song, F. Sun, and K. Iagnemma, “Natural landmark extraction in cluttered forested environments,” in *Proc. 2012 IEEE Int. Conf. Robotics and Automation*, 2012, pp. 4836–4843.
- [10] M. Liu, X. Lei, S. Zhang, and B. Mu, “Natural landmark extraction in 2D laser data based on local curvature scale for mobile robot navigation,” in *Proc. 2010 IEEE Int. Conf. Robotics and Biomimetics*, 2010, pp. 525–530.
- [11] D. Scaramuzza et al., “Vision-controlled micro flying robots: From system design to autonomous navigation and mapping in GPS-denied environments,” *IEEE Robotics & Automation Magazine*, vol. 21, no. 3, pp. 26–40, 2014.
- [12] O. Wijk and H. I. Christensen, “Localization and navigation of a mobile robot using natural point landmarks extracted from sonar data,” *Robotics and Autonomous Systems*, vol. 31, no. 1–2, pp. 31–42, 2000.
- [13] J. H. Ko, W. J. Kim, and M. J. Chung, “A method of acoustic landmark extraction for mobile robot navigation,” *IEEE Transactions on Robotics and Automation*, vol. 12, no. 3, pp. 478–485, 1996.
- [14] N. N. Samany, “Automatic landmark extraction from geo-tagged social media photos using deep neural network,” *Cities*, vol. 93, pp. 1–12, 2019.
- [15] M. Bodini, “A review of facial landmark extraction in 2D images and videos using deep learning,” *Big Data and Cognitive Computing*, vol. 3, no. 1, p. 14, 2019.
- [16] P. Anderson, Y. Yusmanthia, B. Hengst, and A. Sowmya, “Robot localisation using natural landmarks,” in *Proc. Robot Soccer World Cup*, 2012, pp. 118–129.
- [17] J. Aulinas et al., “Feature extraction for underwater visual SLAM,” in *Proc. OCEANS 2011 IEEE-Spain*, 2011, pp. 1–7.
- [18] T. Kim, T.-Y. Lee, and H.-J. Choi, “Landmark extraction, matching, and processing for automated image navigation of geostationary weather satellites,” in *Proc. Image Processing and Pattern Recognition in Remote Sensing II*, vol. 5657, 2005, pp. 30–37.
- [19] W. Zhang, J. Li, Y. Wang, Y. Xiao, P. Liu, and S. Zhang, “A landmark extraction method associated with geometric features and location distribution,” *ISPRS-International Archives of the Photogrammetry, Remote Sensing and Spatial Information Sciences*, pp. 2307–2313, 2018.
- [20] E. Maggiori, Y. Tarabalka, G. Charpiat, and P. Alliez, “Fully convolutional neural networks for remote sensing image classification,” in *Proc. 2016 IEEE Int. Geoscience and Remote Sensing Symp. (IGARSS)*, 2016, pp. 5071–5074.
- [21] Y. Yi, Z. Zhang, and W. Zhang, “Building segmentation of aerial images in urban areas with deep convolutional neural networks,” in *Advances in Remote Sensing and Geo Informatics Applications*, 2019, pp. 61–64.
- [22] S. Wei and M. Lu, “A scale robust convolutional neural network for automatic building extraction from aerial and satellite imagery,” *International Journal of Remote Sensing*, vol. 40, no. 9, pp. 3308–3322, 2019.
- [23] X. Li, Y. Jiang, H. Peng, and S. Yin, “An aerial image segmentation approach based on enhanced multi-scale convolutional neural network,” in *Proc. 2019 IEEE Int. Conf. Industrial Cyber Physical Systems (ICPS)*, 2019, pp. 47–52.
- [24] J. Long, E. Shelhamer, and T. Darrell, “Fully convolutional networks for semantic segmentation,” in *Proc. IEEE Conf. Computer Vision and Pattern Recognition (CVPR)*, 2015, pp. 3431–3440.
- [25] O. Ronneberger, P. Fischer, and T. Brox, “U-Net: Convolutional networks for biomedical image segmentation,” in *Proc. Int. Conf. Medical Image Computing and Computer-Assisted Intervention (MICCAI)*, 2015, pp. 234–241.
- [26] K. He, X. Zhang, S. Ren, and J. Sun, “Deep residual learning for image recognition,” in *Proc. IEEE Conf. Computer Vision and Pattern Recognition (CVPR)*, 2016, pp. 770–778.
- [27] V. Mnih, *Machine Learning for Aerial Image Labeling*, Ph.D. dissertation, Univ. Toronto, Toronto, ON, Canada, 2013.